TECHNICAL NOTE

Analysis of melting in an enclosure with discrete heating at constant rate

Yuwen Zhang, Zhongqi Chen, and Qijie Wang
Department of Power Machinery Engineering, Xi'an Jiaotong University, Xi'an, China

Introduction

Cooling of electronic components has attracted many researchers in the heat transfer field. Natural-convection cooling by ambient air is quite popular because of its simplicity and reliability. Some published papers (Chu and Churchill 1976; Turner and Flack 1980) consider natural convection in an enclosure heated by discrete heat sources. Using solid–liquid phase change materials (PCM) to cool electronic components is a promising alternative for periodically operating apparatus, because phase-change cooling can provide relatively larger cooling capability than air. In accordance with this possibility, experiments were conducted by the present authors for investigating the melting process in an enclosure with one of its side walls discretely heated (Zhang et al. 1993).

Since the shape of the liquid phase is rather irregular during melting, and since the Rayleigh number may be very high (about 10^9), a large amount of computer time is required for the numerical solution of the melting process (Ho and Viskanta 1984). Recently, boundary-layer theory has been adopted by some authors to solve the process of natural-convection-dominated melting. An analytical solution for the melting process in a rectangular enclosure isothermally heated from one of its vertical walls was obtained by Bejan (1989). A similar problem but with a boundary condition of uniform heat flux instead of uniform wall temperature was described by Zhang and Bejan (1989). But to the best of our knowledge, no analytical solution for the above-mentioned melting process with discrete heating has been published yet.

Mathematical model

The experimental enclosure used by Zhang et al. (1993) is schematically shown in Figure 1. Three discrete heat sources made of copper are flush-mounted on the lateral wall, which is made of acrylic Plexiglas. Heat leakage through the back of the lateral wall to the surroundings was minimized by guard heaters, and the whole enclosure was well insulated. The enclosure was filled with n-octadecane. During the beginning stage of the experiment, the surface temperatures of the sources increased gradually, but after a certain time period, they all reached some steady values and remained unchanged. This type of melting process is said to be quasi-steady. Once this state is established, all the heat supplied by the discrete sources will be used to melt the solid phase of PCM at the solid–liquid interface via the natural convection of the liquid phase.

In order to facilitate the solution process, the quasi-steady state is assumed in addition to some classical assumptions, e.g., the initial solid-phase temperature is isothermal and at the melting point. The solution procedure is basically the same as that employed by Bejan (1989), but an important improvement has been made by taking into account the conduction in the discretely heated wall. Since the heat leakage through the back surface of the wall has been minimized, the conduction in the wall can be simplified as a one-dimensional (1-D) steady-state conduction, the dimensionless heat diffusion equation is

$$\frac{d}{dY}\left(K'_w W \frac{d\theta_w}{dY}\right) + Q^* = 0 \tag{1}$$

where K'_w is the dimensionless thermal conductivity of the vertical wall, which equals K_h in the heated section or K_w in

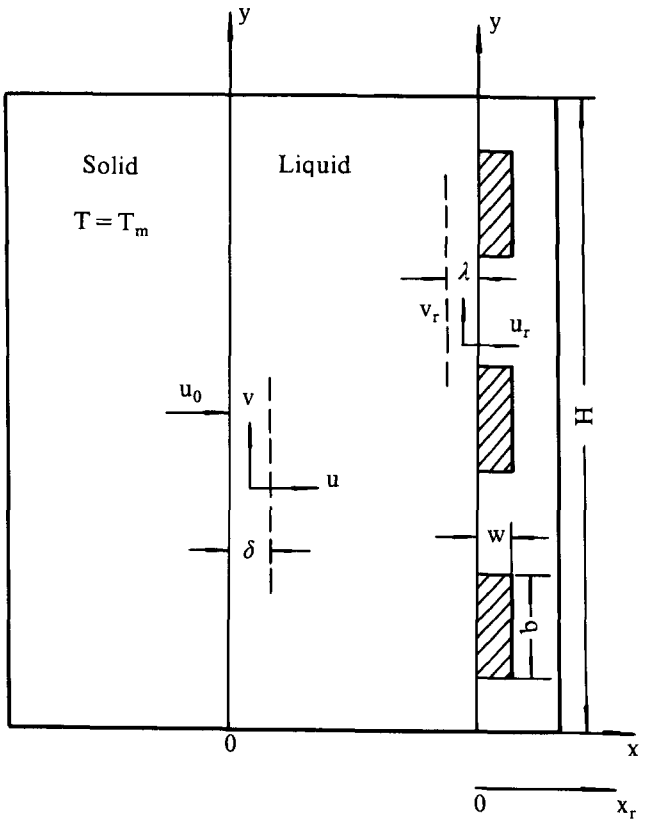

Figure 1 Physical model

Address reprint requests to Professor Zhang at the Department of Power Machinery Engineering, Xi'an Jiaotong University, Xi'an 710049, China.

Received 1 June 1993; accepted 9 September 1993

the unheated section. Q^* is the difference between the amount of heat provided by the discrete sources and the amount transferred to the PCM. This can be expressed as

$$Q^* = \begin{cases} \left(\dfrac{1}{3B} - \dfrac{2(\theta_w - \theta_c)}{\Lambda}\right) \mathrm{Ra}^{1/5} & \text{for the heated section} \\ -\dfrac{2(\theta_w - \theta_c)}{\Lambda} \mathrm{Ra}^{1/5} & \text{for the unheated section} \end{cases} \quad (2)$$

The top and bottom of lateral wall are adiabatic. The boundary conditions, for Equation 1 are

$$\frac{d\theta_w}{dY} = 0, \text{ at } Y = 0 \quad \text{and} \quad 1 \quad (3)$$

Mathematical formulations for the liquid region can be found in Zhang and Bejan's (1989) paper and are omitted here because of space limitations. A numerical method is used to solve these differential equations. The number of nodal points along the height is $N = 900$ in the calculation. The convergence criterion used for both θ_c and θ_w is 10^{-9}.

Results and discussions

The comparison between the predicted and measured dimensionless temperatures of the heated wall when Ste = 2.36 is given in Figure 2. It can be seen that their general tendencies are about the same. Quantitatively speaking, the coincidence of the predicted and measured temperatures on the heat source surface is better than that on the unheated sections (i.e., the surface between the sources). This finding may be attributed to the 1-D simplification of the wall conduction. Compared to the results reported by Zhang and Bejan (1989), temperatures on the heat source surfaces are higher than those for uniform heating, and the reverse is true on the unheated sections. The average temperatures of the heated wall are about the same.

The Stefan number varied from 1.96 to 3.90 during the experiment conducted by Zhang et al. (1993). The computational results show that the dimensionless temperatures of the sources are virtually independent of Ste. So for Ste = 1.96–3.90, the surface temperatures of heat sources T_h can be calculated as

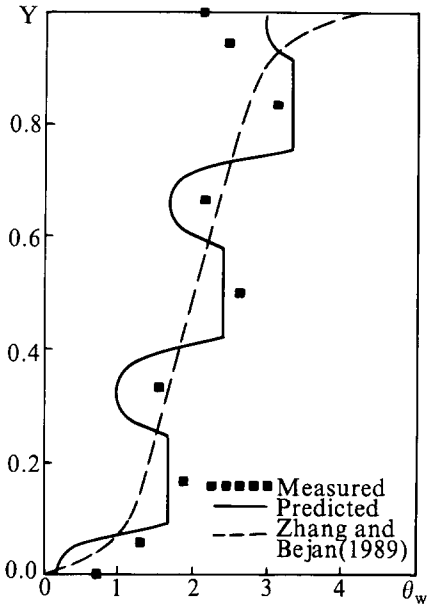

Figure 2 Dimensionless wall temperature

$$(T_h)_n - T_m = A_n \frac{3qb}{k} \mathrm{Ra}^{-1/5} \quad (4)$$

where $n = 1, 2, 3$ represents the lower, middle, and upper heat sources respectively, and A_n's denote corresponding constants, which in that experiment are

$A_1 = 1.67 \quad A_2 = 2.41 \quad A_3 = 3.32$

Notation

b	Height of the heat source
B	Dimensionless height of the heat source, b/H
c_p	Specific heat of liquid
g	Gravitational acceleration
H, L	Height and width of enclosure
h_m	Latent heat
k_h	Thermal conductivity of heated part of the wall
k_l	Thermal conductivity of liquid
k_w	Thermal conductivity of unheated part of the wall
K_h	Dimensionless thermal conductivity of heated part of the wall, k_h/k_l
K_w	Dimensionless thermal conductivity of unheated part of the wall, k_w/k_l
q	Heat flux
Ra	Rayleigh number, $\dfrac{g\beta(3qb/k_l)H^3}{\nu\alpha}$
Ste	Stefan number, $\dfrac{c_p(3qb/k_l)}{h_m}$
T_c	Core temperature
T_m	Melting point
T_w	Wall temperature
U_0	Dimensionless local interface velocity
w	Thickness of discrete sources
W	Dimensionless thickness of discrete sources, w/H
y	Vertical coordinate
Y	Dimensionless vertical coordinate, y/H

Greek symbols

α	Thermal diffusivity of liquid
β	Volumetric thermal expansion coefficient of liquid
δ	Thickness of cold boundary layer
Δ	Dimensionless cold boundary-layer thickness, $\dfrac{\delta}{H}\mathrm{Ra}^{1/5}$
θ_c	Dimensionless core temperature, $\dfrac{(T_c - T_m)}{3qb/k_l}\mathrm{Ra}^{1/5}$
θ_w	Dimensionless wall temperature, $\dfrac{(T_w - T_m)}{3qb/k_l}\mathrm{Ra}^{1/5}$
λ	Thickness of warm boundary layer
Λ	Dimensionless warm boundary-layer thickness, $\dfrac{\lambda}{H}\mathrm{Ra}^{1/5}$
ν	Kinematic viscosity of liquid
ρ	Density of liquid

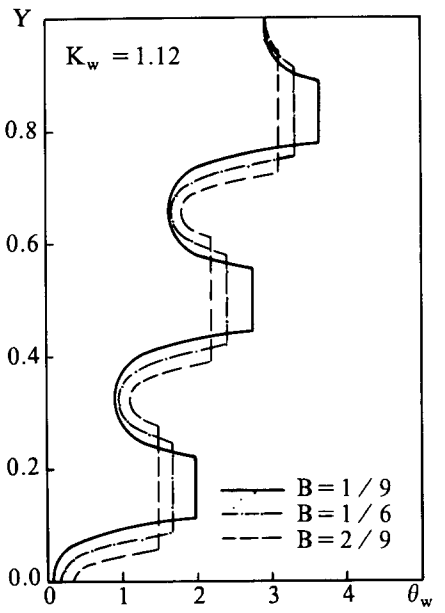

Figure 3 Effect of dimensions of heat sources on the temperature profile

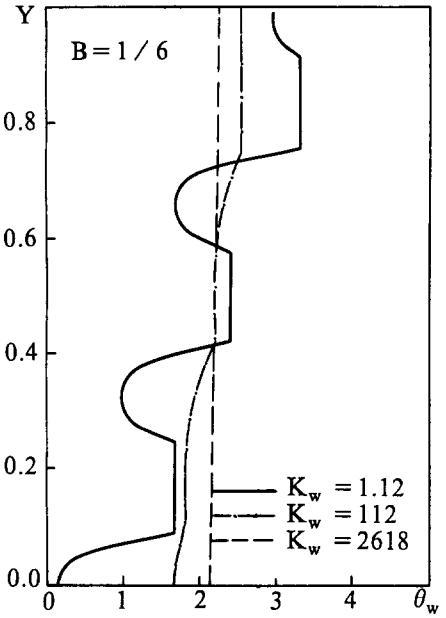

Figure 5 Effect of unheated wall conductivity on the temperature profile

The effect of dimensions of the heat source on the temperature profile in the enclosure is illustrated in Figure 3. As to the effect of the source dimensions, under the same Stefan number (i.e., the power supplied to the discrete source remains unchanged), the larger the height b, the lower the source surface temperature will be. However, the temperature of the unheated section increases. In other words, the temperature difference between the heated and unheated sections will decrease, and then the longitudinal conduction of the wall will decrease as the height of the source increases. The variation of the dimensionless solid–liquid interface velocity along the height of the enclosure with different source heights is shown in Figure 4. This dimensionless velocity can be calculated from the energy conservation at the solid–liquid interface (Bejan 1989), and the result is $U_0(Y) = 2\theta_e(Y)/\Delta(Y)$. From Figure 4, the source height has only a little effect on the interface velocity. The shape of solid–liquid interface becomes more smooth with increasing source height because the temperature difference between the heated section and unheated section becomes smaller.

The variations of wall temperature for different unheated wall conductivities are shown in Figure 5. The surface temperature of the upper source decreases and that of the lower one increases with increasing unheated wall conductivity. The temperatures of the unheated sections are increased as well. The surface temperature distribution of the whole wall tends to be uniform, because the amount of heat flowing downwards through the wall increases with the increasing unheated wall thermal conductivity. Figure 6 shows the variations of the interface moving velocity when the unheated wall conductivity varies. The velocity of the lower interface increases and that of the upper interface decreases as the unheated wall conductivity increases. The reason for this variation is that when unheated

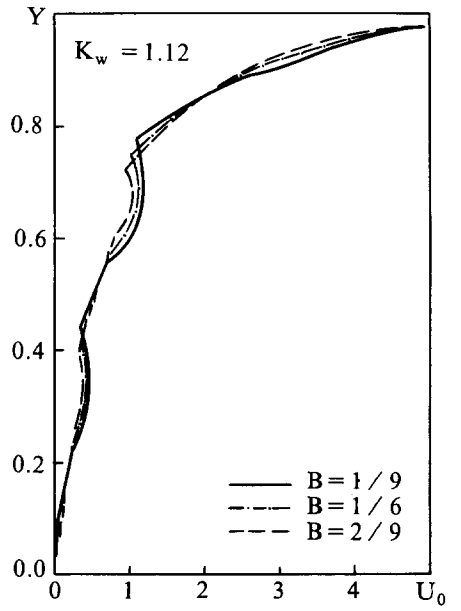

Figure 4 Effect of dimensions of heat sources on the solid–liquid interface velocity

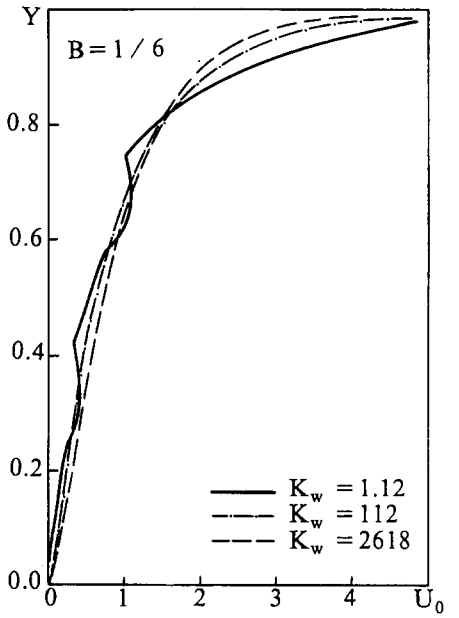

Figure 6 Effect of unheated wall conductivity on the solid–liquid interface velocity

wall conductivity increases, the temperature of the upper part of the wall decreases, but the temperature of the lower part increases.

Acknowledgment

Financial support from the Chinese National Natural Science Foundation is greatly appreciated.

References

Bejan, A. 1989. Analysis of melting by natural convection in an enclosure. *Int. J. Heat Fluid Flow*, **10**, 245–252

Chu, H. H. and Churchill, S. M. 1976. The effect of heater size, location, aspect ratio, and boundary conditions on two-dimensional, laminar, natural convection in rectangular channels. *J. Heat Transfer*, **98**, 194–201

Ho, C. J. and Viskanta, R. 1984. Heat transfer during melting from an isothermal vertical wall. *J. Heat Transfer*, **106**, 12–19

Turner, B. L. and Flack, R. D. 1980. The experimental measurement of natural convection heat transfer in rectangular enclosures with concentrated energy sources. *J. Heat Transfer*, **102**, 236–241

Zhang, Y. W., Chen, Z. Q., Wang, Q. J., and Wu, Q. J. 1993. Melting in an enclosure with discrete heating at constant rate. *Exp. Thermal Fluid Sci.*, **6**, 196–201

Zhang, Z. and Bejan, A. 1989. Melting in an enclosure heated at constant rate. *Int. J. Heat Mass Transfer*, **32**, 1063–1076